IEEE Access
Multidisciplinary | Rapid Review | Open Access Journal

Received January 29, 2021, accepted February 5, 2021, date of publication February 16, 2021, date of current version February 26, 2021.

Digital Object Identifier 10.1109/ACCESS.2021.3059900

Average Dwell Time Based Smooth Switching Linear Parameter-Varying Proportional-Integral-Derivative Control for an F-16 Aircraft

BIXUAN HUANG[1], BEI LU[1], QIFU LI[1], AND YANHUI TONG[2]
[1]School of Aeronautics and Astronautics, Shanghai Jiao Tong University, Shanghai 200240, China
[2]School of Electronic and Electrical Engineering, Shanghai University of Engineering Science, Shanghai 201620, China

Corresponding author: Bei Lu (beilu@sjtu.edu.cn)

This work was supported by the National Natural Science Foundation of China under Grant 61473186.

ABSTRACT Switching control methods have great potential applications in flight control system design. However, nonsmooth control commands at switching instants could lead to performance degradations or bring in safety risks. This paper presents a smooth switching proportional-integral-derivative (PID) control method for linear parameter-varying (LPV) systems to solve this issue. By introducing a transition parameter subspace between any two neighboring LPV subsystems, the switched controller gains are designed to be smoothly varied when the parameter trajectory passes through these subspaces, and the Lyapunov function in the transition subspace is designed independently to make the algorithm less conservatism. The controller synthesis condition is formulated as a linear matrix inequality (LMI) optimization problem using Finsler's lemma. The concept of average dwell-time (ADT) is employed to analyze the performance of the resulting closed-loop system. The effectiveness of the ADT-based smooth switching control strategy is demonstrated by applying it to the nonlinear longitudinal model of the F-16 aircraft, and the simulation results are compared with the traditional ADT switching control method. The results show that the proposed method can achieve a better transition performance with a simpler control structure.

INDEX TERMS Linear parameter-varying systems, proportional-integral-derivative control, average dwell time, smooth-switching control, linear matrix inequalities.

I. INTRODUCTION

In the past decades, the linear parameter-varying (LPV) control technique has been paid great attention in the community of control theory because it provides a theoretical basis for the design of gain-scheduled control systems [1]–[4]. Taking account of the high nonlinearity and time-variability in flight dynamics, the LPV control approach has been extensively applied to the design of flight control systems to reduce conservatism, and see [5]–[8] for instance. The commonly used control structures for the LPV system include the state feedback control and the dynamic output feedback control. It is easy to formulate the LPV state feedback control synthesis problem to a convex linear matrix inequality (LMI) problem, but all the states of the system need to be measurable [9]. To bypass this issue, the LPV dynamic output feedback control can be used, for which the synthesis condition can be rewritten as a set of LMIs by applying elimination lemma [4], [10], [11]. However, a complex controller reconstruction process must be considered after solving the LMI problem. In addition, the resulting dynamic output feedback controller generally has the same order as the generalized open-loop plant, which consists of the controlled system and weighting functions, and thus its order is relatively high. The issues mentioned above motivate researchers to seek more practical and simpler control structures for the LPV systems.

The classical proportional-integral-derivative (PID) control approach with the aid of interpolation is still commonly used in the aviation industry due to its easy implementation. However, the PID control method lacks theoretical guarantees

The associate editor coordinating the review of this manuscript and approving it for publication was Mohammad Alshabi.

for stability and performance for nonlinear systems, and also the associated design process is often time-consuming. In order to integrate the advantages of LPV control and PID control, the analysis and synthesis of multivariable gain scheduled PID control should be conducted using Lyapunov theory [12]. The PID control is first reformulated as a static output feedback control problem [13]. However, the synthesis condition of this problem is a nonconvex bilinear matrix inequality (BMI). Although some nonconvex optimization problem solvers were used to obtain the feasible solution [14] for LPV-PID control, they only suit for the low-order BMIs due to the limitation of solving capabilities [15]. To avoid solving the nonconvex BMI problem directly, the synthesis condition was converted to an LMI problem by adding some constraints, such as assuming the matrix variables are diagonal block matrices [16]. But the shrink of the solution space is inevitable because of the introduced constraint on the structure of matrix variables. Another way is constructing an iterative LMI problem by fixing matrix variables alternately [17], [18], and sometimes it is difficult to obtain a feasible initial solution. In this paper, an LMI synthesis condition with full matrix variables is proposed for LPV-PID control, and it is computationally less complicated than iterative methods.

On the other hand, because a flight control system involves a large flight envelop, it is sometimes difficult to find a single LPV controller to stabilize the system in the entire parameter space. Thus, the switching LPV control method was proposed [19], which consists of several LPV controllers, each designed for a certain parameter subspace. The system is switched depending on the current system parameters, i.e., when the trajectory of the parameter hits the switching surface and gets to the adjacent parameter subspace, the controller for this subsystem is activated. The commonly used switching LPV control methods include hysteresis switching and switching with an average dwell time (ADT). Using the characteristics of switching logic to design the Lyapunov functions, the stability of the system can be guaranteed. These methods were applied to the F-16 aircraft with a wide angle of attack variation [5], [19], and the results demonstrated that switching LPV control can improve the system performance as well as the design flexibility. Since the switching LPV control method was first proposed, it has been improved continuously [20]–[23], for instance, considering the influence of parametric uncertainties, rejecting the disturbances, optimizing the switching surfaces, etc.

However, the traditional switching LPV control only seeks the stability and performance of the system under the constrained switching signal, and does not consider the transition performance at switching surfaces. The controllers are simply assumed to be directly switched from one to another. This type of switching will generate a nonsmooth control command at switching surfaces, and will possibly lead to actuator saturations, mechanical damages, and even safety risks for aircraft. To obtain a better transition performance, some smooth switching control methods are developed. The interpolation-based smooth switching methods were proposed [24], [25], where overlapped parameter spaces were constructed between adjacent subspaces, and LPV controllers for these overlapped regions were obtained by linearly interpolating the control gains of the adjacent subspaces. Based on the first-order interpolation, these methods were extended to a higher-order differentiable control signal by introducing a description of the "smoothness" of the controller in the matrix norm [26]. However, for most interpolation methods, the Lyapunov functions for the overlapped parameter spaces are obtained by interpolating those of the adjacent subspaces, and this increases the conservatism of the algorithm. On the other hand, the changes of control input at switching surfaces are limited by adding a soft constraint [7] or a bumpless transfer constraint [27]. But these constraints also lead to similar control gains for different subspaces, and thus the performance in each subspace is not optimal. In this paper, the interpolation method is used, but the Lyapunov function in the overlapped subsystem (or the transition subsystem) is designed independently.

Based on the above-mentioned background, in this paper, we propose a smooth switching LPV-PID control design method, which has a simple PID control structure and achieves a smooth transition performance. The proposed method is applied to the longitudinal motion control of aircraft over a wide range of airspeed. The main contributions of this paper can be summarized as follows:

1) The switching LPV controller is designed in a PID structure to reduce the application complexity.
2) The switching surfaces are replaced by transition subspaces to achieve the smooth control command, and the independent Lyapunov functions are designed for each transition subspace to reduce the conservatism.
3) The synthesis condition for smooth switching LPV-PID control is formulated as an LMI problem with full matrix variables to avoid solving the BMI problem.

This paper is organized as follows. The switching LPV-PID control system and the control requirements are first described in Section 2. Then, the formulation of the closed-loop system and synthesis conditions are provided in Section 3. The proposed method is applied to the longitudinal autopilot system, and the nonlinear simulation results are shown in Section 4. Section 5 concludes the paper.

The notation in this paper is fairly standard. $\mathbb{R}$ stands for the set of real numbers. $\mathbb{R}^{m\times n}$ denotes the set of real $m \times n$ matrices. Hermitian operator $\mathrm{Her}\{\cdot\}$ is denoted as $\mathrm{Her}\{A\} = A+A^T$ for real matrices. M^T and M^{-1} represent the transpose and inverse of a matrix, respectively. $M > 0$ ($M \geq 0$) denotes a positive definite (semidefinite) matrix, and $M < 0$ ($M \leq 0$) denotes a negative definite (semidefinite) matrix. $\mathbb{R}^n$ stands for an n -dimensional Euclidean space, and $\|\cdot\|$ denotes the Euclidean norm of a vector. The space of square-integrable functions is expressed as L_2, and its norm for $w \in L_2$ is $\|w\|_2 = \sqrt{\int_0^\infty w^T(t)w(t)dt}$. $diag\{M_1, M_2, \ldots, M_n\}$ denotes a block diagonal matrix with submatrices $M_1, M_2, \ldots, M_n$.

II. PROBLEM DESCRIPTION

A. DESCRIPTION OF THE LPV SYSTEM

Consider a smooth switching LPV-PID control system as shown in Fig. 1, where the plant $P(\rho)$ can be represented as the following LPV model.

$$\begin{bmatrix} \dot{x} \\ z \\ y \end{bmatrix} = \begin{bmatrix} A(\rho) & B_w(\rho) & B_u(\rho) \\ C_z(\rho) & D_{zw}(\rho) & D_{zu}(\rho) \\ C_y & 0 & 0 \end{bmatrix} \begin{bmatrix} x \\ w \\ u \end{bmatrix} \tag{1}$$

where the vectors $x \in \mathbb{R}^n$, $u \in \mathbb{R}^{n_u}$, $y \in \mathbb{R}^{n_y}$, and $z \in \mathbb{R}^{n_z}$ are the state, the control input, the measured output and the performance output, respectively. The vector $w = \begin{bmatrix} w_0^T & r^T \end{bmatrix}^T \in \mathbb{R}^{n_w}$ is the exogenous input including the disturbance w_0 and the reference r, and the related input matrix is partitioned accordingly, i.e., $B_w(\rho) = \begin{bmatrix} B_{w1}(\rho) & B_{w2}(\rho) \end{bmatrix}$.

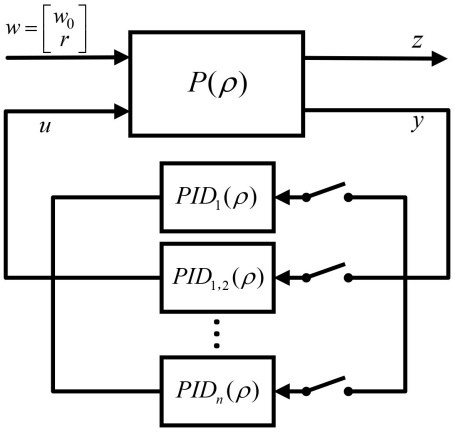

FIGURE 1. Generic framework of smooth switching LPV-PID control.

The vector of scheduling parameter ρ belongs to a compact set $\mathcal{P} \subset \mathbb{R}^s$, and its time derivative is in a set $\mathcal{V} \subset \mathbb{R}^s$, where $\mathcal{P} := \{\underline{\rho}_j \le \rho_j \le \bar{\rho}_j\}$, $\mathcal{V} := \{\underline{v}_j \le \dot{\rho}_j \le \bar{v}_j\}$, $j = 1, 2 \ldots, s$. The parameters are measurable in real time. To design the switching control system, assume the parameter space $\mathcal{P}$ is divided into $2m-1$ subspaces along one parameter axis ρ_r, $r \in \{1, 2 \ldots, s\}$, where the subspaces can be represented as:

$$\Theta_i = \{\rho \in \Theta | \underline{\rho}_{i,r} \le \rho_r \le \overline{\rho}_{i,r}\}, \quad i = 1, 2, \ldots, m, \tag{2}$$

$$\Theta_{i,i+1} = \{\rho \in \Theta | \bar{\rho}_{i,r} \le \rho_r \le \underline{\rho}_{i+1,r}\}, \quad i = 1, 2, \ldots, m-1. \tag{3}$$

In Fig. 2, a two-dimensional parameter space is shown as an example. Between every two normal subspaces Θ_i and Θ_{i+1}, there exists a transition subspace $\Theta_{i,i+1}$, which can be regarded as an extension of a switching surface, and the relations between these sets can be expressed as

$$\mathcal{P} = \left(\cup_{i=1}^{m} \Theta_i\right) \cup \left(\cup_{i=1}^{m-1} \Theta_{i,i+1}\right).$$

Accordingly, the LPV system in (1) can be written in a partitioned form

$$\begin{bmatrix} \dot{x} \\ z \\ y \end{bmatrix} = \begin{bmatrix} A_j(\rho) & B_{w,j}(\rho) & B_{u,j}(\rho) \\ C_{z,j}(\rho) & D_{zw,j}(\rho) & D_{zu,j}(\rho) \\ C_{y,j} & 0 & 0 \end{bmatrix} \begin{bmatrix} x \\ w \\ u \end{bmatrix} \tag{4}$$

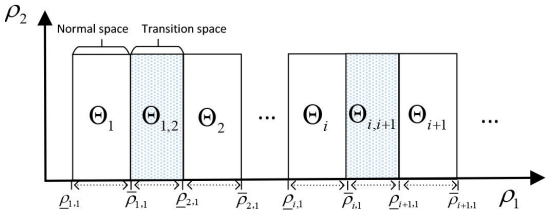

FIGURE 2. Partition of a two-dimensional parameter space along one axis.

where the subscript j indicates the corresponding subspace, i.e., $j = i$ means $\rho \in \Theta_i$, and $j = (i, i+1)$ means $\rho \in \Theta_{i,i+1}$.

For each partitioned subspace, a smooth switching gain-scheduled PID controller is designed as follow.

$$u = K_{P,j}(\rho)y + K_{I,j}(\rho)x_I + K_{D,j}(\rho)G_D\frac{dy}{dt}, \tag{5}$$

where G_D is a matrix selecting the signals from the vector y, the state of the integrator is

$$x_I = \int_0^t (G_r w - G_I x)dt \in \mathbb{R}^{ni}, \tag{6}$$

G_r is a matrix extracting the reference signal r from the vector w. The definition of smooth switching represents that the control gains $K_{P,j}(\rho)$, $K_{I,j}(\rho)$, $K_{D,j}(\rho)$ are continuous in the entire parameter space, i.e., $K_{*,i}(\underline{\rho}_{i,r}) = K_{*,(i-1,i)}(\underline{\rho}_{i,r})$, and $K_{*,i}(\bar{\rho}_{i,r}) = K_{*,(i,i+1)}(\bar{\rho}_{i,r})$, where K_* represents the control gains K_P, K_I, and K_D. The controllers for Θ_i are local LPV controllers, which only take charge of the stability and performance of the subsystems Θ_i. The controller for the subspace $\Theta_{i,i+1}$ not only plays a control role, but also has a smooth effect to make the control gains change continuously from Θ_i to Θ_{i+1} or vice versa.

Note that the structure of the designed PID controller is slightly different from the typical PID controller. First, a more general form of error, $r - G_I x$, is used instead of r-y, where $G_I x$ is a matrix extracting the corresponding tracking signal from the state vector x. For example, if an ideal model is used, the error between the ideal output and the measured output involves the reference and states of the ideal model and the plant. Then the expression $G_r w - G_I x$ can be used to represent the tracking error. Second, for the convenience of designing a multi-input multi-output controller, the output vector y is used in the proportional term to provide more information to the controller.

Remark 1: The output matrix C_y is assumed as a constant matrix. On one hand, it is usually true in most real applications. On the other hand, this assumption eliminates the need to obtain the derivative of $C_y(\rho)$ for PID control design. It should be pointed out that the output matrix C_y can be assumed as a parameter-dependent matrix if PI control is used.

B. DESCRIPTION OF THE SWITCHING PROBLEM

To describe the switching logic, an index set of the subspaces is defined as

$$Z_M := \{j | j = i, i \in \{1, 2, \ldots, m\}, \text{or } j = (i, i+1), \\ i \in \{1, 2, \ldots, m-1\}\}. \quad (7)$$

A mapping $\sigma : [0, \infty) \to Z_M$ is defined to indicate the activated subsystem. The value of σ depends on time and subspaces where the parameter ρ is located.

As shown in Fig. 3, if the trajectory of parameter moves from Θ_i to $\Theta_{i,i+1}$ and hits the surface $\bar{\rho}_{i,r}$, the value of σ changes from i to $(i, i+1)$ and the controller for $\Theta_{i,i+1}$ is activated. Then, if the trajectory of parameter continuously changes through subspace $\Theta_{i,i+1}$, the control gains begin to smoothly change to the controller for Θ_{i+1}. The opposite movement has the similar situation.

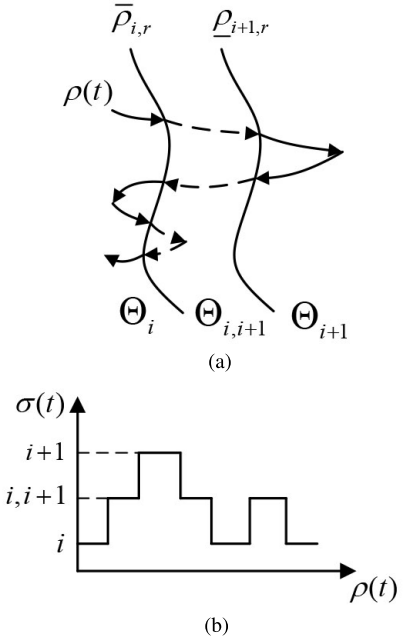

FIGURE 3. (a) Smooth switching region; (b) the corresponding value of σ.

Before proposing the control objective, a definition of weighted L_2 performance is given to characterize the system performance.

Definition 2: [28] For $\beta > 0$ and $\gamma > 0$, the system is said to have a bounded weighted L_2-gain γ if the following inequality holds for zero initial condition $x(0) = 0$.

$$\int_0^\infty e^{-\beta t} z^T(t) z(t) dt \le \gamma^2 \int_0^\infty w^T(t) w(t) dt. \quad (8)$$

The control objective of this work is to design a smooth switching LPV-PID controller (5) for the open-loop system (4), to satisfy following requirements.

1) The asymptotic stability of the closed-loop system can be guaranteed.
2) The weighted L_2-gains of the closed-loop system are bounded.
3) The controller gains can switch smoothly between normal and transitional subspaces.
4) The Lyapunov function for each subsystem is designed to be independent to reduce the conservatism.

III. CONTROLLER SYNTHESIS

A. FORMULATION OF THE CLOSED-LOOP SYSTEM

In this section, to construct the closed-loop system, the plant (4) and controller (5) are reformulated to an augmented form. Moreover, the specific representation of the smooth switching PID controller is provided.

The state of the plant x is combined with the state of the integrator x_I to construct an augmented state

$$\bar{x} = [\, x^T \quad x_I^T \,]^T.$$

The state-space model of the augmented plant is given by the following equation.

$$\begin{bmatrix} \dot{\bar{x}} \\ z \end{bmatrix} = \begin{bmatrix} \bar{A}_j(\rho) & \bar{B}_{w,j}(\rho) & \bar{B}_{u,j}(\rho) \\ \bar{C}_{z,j}(\rho) & \bar{D}_{zw,j}(\rho) & \bar{D}_{zu,j}(\rho) \end{bmatrix} \begin{bmatrix} \bar{x} \\ w \\ u \end{bmatrix} \quad (9)$$

where

$$\bar{A}_j(\rho) = \begin{bmatrix} A_j(\rho) & 0 \\ -G_I & 0 \end{bmatrix}, \quad \bar{B}_{u,j}(\rho) = \begin{bmatrix} B_{u,j}(\rho) \\ 0 \end{bmatrix},$$
$$\bar{B}_{w,j}(\rho) = \begin{bmatrix} B_{w,j}(\rho) \\ G_r \end{bmatrix}, \quad \bar{C}_{z,j}(\rho) = \begin{bmatrix} C_{z,j}(\rho) & 0 \end{bmatrix},$$
$$\bar{D}_{zu,j}(\rho) = D_{zu,j}(\rho), \quad \bar{D}_{zw,j}(\rho) = D_{zw,j}(\rho).$$

The smooth switching PID controller is also reformulated as the following equation using the augmented state.

$$\begin{aligned} u &= \bar{K}_j(\rho)\bar{y} \\ &= \bar{K}_j(\rho) \begin{bmatrix} \bar{C}_{y,j}(\rho) & \bar{D}_{y,j}(\rho) \end{bmatrix} \begin{bmatrix} \bar{x} \\ w \end{bmatrix}, \end{aligned} \quad (10)$$

where

$$\bar{C}_{y,j}(\rho) = \begin{bmatrix} C_{y,j} & 0 \\ 0 & I \\ G_D C_{y,j} A_j(\rho) & 0 \end{bmatrix},$$
$$\bar{D}_{y,j}(\rho) = \begin{bmatrix} 0 \\ 0 \\ G_D C_{y,j} B_{w,j}(\rho) \end{bmatrix},$$
$$\bar{K}_j(\rho) = \begin{bmatrix} \bar{K}_{P,j}(\rho), \bar{K}_{I,j}(\rho), \bar{K}_{D,j}(\rho) \end{bmatrix}, \quad (11)$$

with

$$\bar{K}_{P,j}(\rho) = (I - K_{D,j}(\rho) G_D C_{y,j} B_{u,j}(\rho))^{-1} K_{P,j}(\rho),$$
$$\bar{K}_{I,j}(\rho) = (I - K_{D,j}(\rho) G_D C_{y,j} B_{u,j}(\rho))^{-1} K_{I,j}(\rho),$$
$$\bar{K}_{D,j}(\rho) = (I - K_{D,j}(\rho) G_D C_{y,j} B_{u,j}(\rho))^{-1} K_{D,j}(\rho).$$

If the continuous function of control gain $\bar{K}_j(\rho)$ is obtained, the gains for PID controller in (5) can be formulated by following expressions. Considering the continuity of system

matrices $C_{y,j}$ and $B_{u,j}(\rho)$, the smoothness of control gains can be guaranteed.

$$\begin{aligned} K_{D,j}(\rho) &= \bar{K}_{D,j}(\rho)(I + G_D C_{y,j} B_{u,j}(\rho)\bar{K}_{D,j}(\rho))^{-1}, \\ K_{P,j}(\rho) &= (I - K_{D,j}(\rho) G_D C_{y,j} B_{u,j}(\rho))\bar{K}_{P,j}(\rho), \\ K_{I,j}(\rho) &= (I - K_{D,j}(\rho) G_D C_{y,j} B_{u,j}(\rho))\bar{K}_{I,j}(\rho), \end{aligned} \tag{12}$$

The control gain matrix $\bar{K}_j(\rho)$ is designed as

$$\bar{K}_j(\rho) = M_j(\rho) X_j^{-1}(\rho), \tag{13}$$

where $j = i$ or $(i, i+1)$. The matrices $X_j(\rho)$ and $M_j(\rho)$ are introduced here to give an explicit expression of the smooth switching control gain matrix. They will appear as LMI variables in the control synthesis conditions and the detailed derivation will be given later.

For normal subspaces Θ_i, we assume

$$M_i(\rho) = M_i(\rho) \quad \rho \in \Theta_i, \tag{14}$$

$$X_i(\rho) = X_i(\rho) \quad \rho \in \Theta_i. \tag{15}$$

For transitional subspaces $\Theta_{i,i+1}$, the matrices $M_{i,i+1}(\rho)$ and $X_{i,i+1}(\rho)$ are defined as a function of $M_i(\rho)$ and $X_i(\rho)$ to smooth the gains of the controller. In our case, this function is a linear function depending on the parameter ρ_r.

$$M_{i,i+1}(\rho) = \alpha_1 M_i(\rho) + \alpha_2 M_{i+1}(\rho), \quad \rho \in \Theta_{i,i+1}, \tag{16}$$

$$X_{i,i+1}(\rho) = \alpha_1 X_i(\rho) + \alpha_2 X_{i+1}(\rho), \quad \rho \in \Theta_{i,i+1}, \tag{17}$$

where $\alpha_1 = \frac{\rho_{i+1,r} - \rho_r}{\rho_{i+1,r} - \overline{\rho}_{i,r}}$, $\alpha_2 = 1 - \alpha_1$.

Combining the augmented open-loop LPV system (9) and the reformulated controller (10), the switched closed-loop system under a switching signal σ can be expressed as the following state-space model.

$$\begin{aligned} \dot{\bar{x}}_\sigma &= \underbrace{\left(\bar{A}_\sigma(\rho) + \bar{B}_{u,\sigma}(\rho)\bar{K}_\sigma(\rho)\bar{C}_{y,\sigma}(\rho)\right)}_{A_{cl,\sigma}}\bar{x} \\ &\quad + \underbrace{\left(\bar{B}_{w,\sigma}(\rho) + \bar{B}_{u,\sigma}(\rho)\bar{K}_\sigma(\rho)\bar{D}_{y,\sigma}(\rho)\right)}_{B_{cl,\sigma}} w, \\ z &= \underbrace{\left(\bar{C}_{z,\sigma}(\rho) + \bar{D}_{zu,\sigma}(\rho)\bar{K}_\sigma(\rho)\bar{C}_{y,\sigma}(\rho)\right)}_{C_{cl,\sigma}}\bar{x} \\ &\quad + \underbrace{\left(\bar{D}_{zw,\sigma}(\rho) + \bar{D}_{zu,\sigma}(\rho)\bar{K}_\sigma(\rho)\bar{D}_{y,\sigma}(\rho)\right)}_{D_{cl,\sigma}} w. \end{aligned} \tag{18}$$

B. FORMULATION OF SYNTHESIS CONDITIONS

Before giving the synthesis condition of the smooth switching LPV-PID controller, an ADT constraint is introduced for the switching signal σ to help analyzing the system performance subsequently. Also, Finsler's lemma is given below, which plays an important role in our approach.

Definition 3 [29]: Let $N_\sigma(t_1, t_2)$ be the switching number of switching signal $\sigma(t)$ in an interval $t_2 > t_1 > 0$. If the following inequality

$$N_\sigma(t_1, t_2) \le N_0 + \frac{t_2 - t_1}{\tau_a} \tag{19}$$

holds for given $N_0 > 0$ and $\tau_a > 0$, then the constants τ_a and N_0 are called an average dwell time and a chatter bound, respectively.

Lemma 4 (Finsler): [30] Let $Z \in \mathbb{R}^{m\times m}$ a symmetric matrix, $V \in \mathbb{R}^{n\times m}$ such that $rank(V) \le m$. The following statements are equivalent:

1) There exists a matrix $\Delta \in \mathbb{R}^{m\times n}$

$$Z + \Delta V + V^T \Delta^T < 0, \tag{20}$$

2)

$$N_V^T Z N_V < 0, \tag{21}$$

where N_V is a matrix whose columns form the bases of the null space of V.

Before providing the synthesis condition, the criteria for Lyapunov functions to guarantee the requirements defined in Section 2.2 are first developed for the closed-loop system (18).

Lemma 5: For the closed-loop system (18), if there exist constants $\beta > 0$, $\mu > 1$, $\gamma > 0$ and a set of Lyapunov functions $V_j(\rho, t)$ for parameter subspaces Θ_j, $j = i$ or $(i, i+1)$, such that

1) $\forall t \in [t_{n-1}, t_n)$, $\rho \in \Theta_i$

$$\dot{V}_i(\rho, t) \le -\beta V_i(\rho, t) - \frac{1}{\gamma} z^T z + \gamma w^T w, \tag{22}$$

2) $\forall t \in [t_n, t_{n+1})$, $\rho \in \Theta_{i,i+1}$

$$\dot{V}_{i,i+1}(\rho, t) \le -\beta V_{i,i+1}(\rho, t) - \frac{1}{\gamma} z^T z + \gamma w^T w, \tag{23}$$

3) $\forall \sigma(t_n) = i, \sigma(t_n^-) = i, i+1, \rho \in \Theta_i \cap \Theta_{i,i+1}$

$$V_{i,i+1}(\rho, t_n) \le \mu V_i(\rho, t_n^-), \tag{24}$$

4) $\forall \sigma(t_n) = i, i+1, \sigma(t_n^-) = i, \rho \in \Theta_i \cap \Theta_{i,i+1}$

$$V_i(\rho, t_n) \le \mu V_{i,i+1}(\rho, t_n^-), \tag{25}$$

where t_{n-1}, t_n and t_{n+1} are switching instants, t_n^- is the instant before switching. Then, the closed-loop system for any scheduling parameter ρ is asymptotically stable with the weighted L_2-gain performance $\gamma\mu^{N_0/2}$ guaranteed for any switching signal σ with ADT $\tau_a > \frac{\ln \mu}{\beta}$.

Proof: According to the requirement (iv) in Section 2.2, independent Lyapunov functions $V_i(\rho, t)$ and $V_{i,i+1}(\rho, t)$ are considered for corresponding Θ_i and $\Theta_{i,i+1}$ subspaces.

To analyze the stability of the system, let $w = 0$, and the inequalities (22) and (23) can be written as

$$\dot{V}_j(\rho, t) \le -\beta V_j(\rho, t) - \frac{1}{\gamma} z^T z \le 0, \tag{26}$$

where $j = i$ or $(i, i+1)$. This implies that the system stability in parameter subspaces Θ_i and $\Theta_{i,i+1}$ can be guaranteed.

Then, consider the stability of the switched system with a switching signal σ under ADT constraints. Let initial time $t_0 = 0$ and $t_1 < t_2 < \ldots < t_n$ as the switching time instants, where $n = N_\sigma(0, t)$ is the number of switching. The

Lyapunov function at time t satisfies the following condition in any of subsystems Θ_i or $\Theta_{i,i+1}$.

$$V_\sigma(\rho,t) \le e^{-\beta(t-t_n)}V_\sigma(\rho,t_n), \forall t \in [t_n, t_{n+1}). \tag{27}$$

Combining with (24) and (25), the Lyapunov function at time t satisfies

$$\begin{aligned} V_\sigma(\rho,t) &\le e^{-\beta(t-t_n)}V_\sigma(\rho,t_n) \le \mu e^{-\beta(t-t_n)}V_\sigma(\rho,t_n^-) \\ &\le \ldots \le \mu^{N_\sigma(0,t)}e^{-\beta t}V_\sigma(\rho,0) \\ &\le \mu^{N_0}e^{(\frac{\ln\mu}{\tau_a}-\beta)t}V_\sigma(\rho,0), \end{aligned} \tag{28}$$

where t_n^- is the time instant before switching. For any switching signal with ADT satisfying $\frac{\ln\mu}{\tau_a} - \beta < 0$, the Lyapunov function $V_\sigma(\rho,t)$ converges to zero when $t \to \infty$, and therefore the system is asymptotically stable.

Next, to analyze the robust performance of the closed-loop system, we integrate (22) and (23) and get the following inequality

$$\begin{aligned} V_\sigma(\rho,t) \le\ & e^{-\beta(t-t_n)}V_\sigma(\rho,t_n) \\ & - \int_{t_n}^{t} e^{-\beta(t-\tau)}\Gamma(\tau)d\tau, t \in [t_n, t_{n+1}), \end{aligned} \tag{29}$$

where $\Gamma(\tau) = \frac{1}{\gamma}z^T(\tau)z(\tau) - \gamma w^T(\tau)w(\tau)$. According to (24) and (25), from $t_0 = 0$ to an arbitrary time instant t, there is

$$\begin{aligned} V_\sigma(\rho,t) &\le \mu e^{-\beta(t-t_n)}V_\sigma(\rho,t_n^-) - \int_{t_n}^{t} e^{-\beta(t-\tau)}\Gamma(\tau)d\tau \\ &\le \mu e^{-\beta(t-t_n)}\Big[e^{-\beta(t_n-t_{n-1})}V_\sigma(\rho,t_{n-1}) \\ &\qquad - \int_{t_{n-1}}^{t_n} e^{-\beta(t_n-\tau)}\Gamma(\tau)d\tau\Big] \\ &\qquad - \int_{t_n}^{t} e^{-\beta(t-\tau)}\Gamma(\tau)d\tau \\ &\quad \vdots \\ &\le \mu^n e^{-\beta t}V_\sigma(\rho,0) - \mu^n\int_0^{t_1} e^{-\beta(t-\tau)}\Gamma(\tau)d\tau - \ldots \\ &\quad - \mu^0\int_{t_n}^{t} e^{-\beta(t-\tau)}\Gamma(\tau)d\tau \\ &= \mu^{N_\sigma(0,t)}e^{-\beta t}V_\sigma(\rho,0) \\ &\quad - \int_0^t \mu^{N_\sigma(\tau,t)}e^{-\beta(t-\tau)}\Gamma(\tau)d\tau. \end{aligned} \tag{30}$$

Because $V_\sigma(\rho,0) = 0$, multiplying both sides of (30) by $\mu^{-N_\sigma(0,t)}$ yields

$$\int_0^t \mu^{-N_\sigma(0,\tau)}e^{-\beta(t-\tau)}\Gamma(\tau)d\tau \le -\mu^{-N_\sigma(0,t)}V_\sigma(\rho,t) \le 0 \tag{31}$$

If the ADT constraint is satisfied, we have $N_\sigma(0,\tau)\ln\mu \le N_0\ln\mu + \beta\tau$, and then (31) can be reconstructed as

$$\begin{aligned} &\mu^{-N_0}\int_0^t e^{-\beta\tau}e^{-\beta(t-\tau)}z^T(\tau)z(\tau)d\tau \\ &\qquad \le \gamma^2\int_0^t e^{-\beta(t-\tau)}w^T(\tau)w(\tau)d\tau. \end{aligned} \tag{32}$$

Integrating both sides of (32) gives

$$\begin{aligned} &\mu^{-N_0}\int_0^\infty\int_0^t e^{-\beta\tau}e^{-\beta(t-\tau)}z^T(\tau)z(\tau)d\tau dt \\ &= \mu^{-N_0}\int_0^\infty e^{-\beta\tau}z^T(\tau)z(\tau)\left(\int_\tau^\infty e^{-\beta(t-\tau)}dt\right)d\tau \\ &= \mu^{-N_0}/\beta\int_0^\infty e^{-\beta\tau}z^T(\tau)z(\tau)d\tau \\ &\le \gamma^2\int_0^\infty w^T(\tau)w(\tau)\left(\int_\tau^\infty e^{-\beta(t-\tau)}dt\right)d\tau \\ &= \gamma^2/\beta\int_0^\infty w^T(\tau)w(\tau)d\tau, \end{aligned} \tag{33}$$

which implies that

$$\int_0^\infty e^{-\beta\tau}z^T(\tau)z(\tau)d\tau \le \left(\gamma\mu^{N_0/2}\right)^2\int_0^\infty w^T(\tau)w(\tau)d\tau. \tag{34}$$

Hence, the weighted L_2-gain of the closed-loop system is bounded by $\gamma\mu^{N_0/2}$.

Remark 6: Consider the Lyapunov function $V_i(\rho,t) = \bar{x}^TP_i(\rho)\bar{x}$. Substituting the closed-loop state-space matrices into (22) yields the following inequality.

$$\begin{aligned} &\begin{bmatrix} \mathrm{Her}\{P_i(\rho)A_{cl,i}(\rho)\} + \dfrac{\partial Pi}{\partial\rho}\dot{\rho} + \beta P_i(\rho) & * \\ B_{cl,i}^TP_i(\rho) & -\gamma \end{bmatrix} \\ &\quad + \frac{1}{\gamma}\begin{bmatrix} C_{cl,i}^T(\rho) \\ D_{cl,i}^T(\rho) \end{bmatrix}\begin{bmatrix} C_{cl,i}(\rho) & D_{cl,i}(\rho) \end{bmatrix} \le 0 \end{aligned} \tag{35}$$

where

$$P_i(\rho)A_{cl,i}(\rho) = P_i(\rho)\bar{A}_i(\rho) + P_i(\rho)\bar{B}_{u,i}(\rho)\bar{K}_i(\rho)\bar{C}_{y,i}(\rho). \tag{36}$$

Note that (35) is a BMI problem, because the term $P_i(\rho)\bar{B}_{u,i}(\rho)\bar{K}_i(\rho)\bar{C}_{y,i}(\rho)$ involves Lyapunov function matrix $P_i(\rho)$ and control gain matrix $\bar{K}_i(\rho)$, both of which are unknown in the control synthesis problem. Similar problems also exist in other conditions of Lemma 5.

In following Theorem, using Finsler's lemma, an LMI synthesis condition of controller (10) for the closed-loop system (18) under the ADT switching signal is presented.

Theorem 7: Consider the open-loop system in (9), if there exist parameter dependent symmetric positive-definite matrices $Q_i(\rho) \in \mathbb{R}^{(n+ni)\times(n+ni)}$ and $Q_{i,i+1}(\rho) \in \mathbb{R}^{(n+ni)\times(n+ni)}$, full matrices $M_j(\rho) \in \mathbb{R}^{n_u\times n_{\bar{y}}}$ and $X_j(\rho) \in \mathbb{R}^{n_{\bar{y}}\times n_{\bar{y}}}$, and given scalars $\beta > 0$, $\mu > 1$ and $\varepsilon > 0$, such that the following optimization problem with $\gamma > 0$ is solvable for any scheduling parameter ρ.

$$\min \gamma, \tag{37}$$

$$\Pi_i < 0 \quad \rho \in \Theta_i, \tag{38}$$

$$\Pi_{i,i+1} < 0 \quad \rho \in \Theta_{i,i+1}, \tag{39}$$

$$\begin{aligned} \frac{1}{\mu}Q_{i,i+1}(\rho) \le Q_i(\rho) \le \mu Q_{i,i+1}(\rho) \\ \rho \in \Theta_{i,i+1} \cap \Theta_i, \end{aligned} \tag{40}$$

$$\Pi_j = \begin{bmatrix} \Phi_{11} & * & * & * \\ \bar{B}_{w,j}^T(\rho) & -\gamma I & * & * \\ \Phi_{31} & \bar{D}_{zw,j}(\rho) & -\gamma I & * \\ \Phi_{41} & \bar{D}_{y,j}(\rho) & \Phi_{43} & \Phi_{44} \end{bmatrix}, \tag{41}$$

where

$$\begin{aligned}
\Phi_{11} &= \mathrm{Her}\{\bar{A}_j(\rho)Q_j(\rho) + \bar{B}_{u,j}(\rho)M_j(\rho)\bar{C}_{y,j}(\rho)\} \\
&\quad - \frac{\partial Q_j}{\partial \rho}\dot{\rho} + \beta Q_j(\rho), \\
\Phi_{31} &= \bar{C}_{z,j}(\rho)Q_j(\rho) + \bar{D}_{zu,j}(\rho)M_j(\rho)\bar{C}_{y,j}(\rho), \\
\Phi_{41} &= \bar{C}_{y,j}(\rho)Q_j(\rho) - X_j(\rho)\bar{C}_{y,j}(\rho) + \varepsilon M_j^T(\rho)\bar{B}_{u,j}^T(\rho), \\
\Phi_{43} &= \varepsilon M_j^T(\rho)\bar{D}_{zu,j}^T(\rho), \\
\Phi_{44} &= -\varepsilon \mathrm{Her}\{X_j(\rho)\},
\end{aligned}$$

$j = i$, or $i, i+1$ is the index of subspaces. The expressions of $M_{i,i+1}(\rho) \in \mathbb{R}^{n_u \times n_{\bar{y}}}$ and $X_{i,i+1}(\rho) \in \mathbb{R}^{n_{\bar{y}} \times n_{\bar{y}}}$ are given in (16) and (17). Then, the closed-loop system with the smooth switching controller (5) is asymptotically stable with the weighted L_2 -gain performance $\gamma\mu^{N_0/2}$ guaranteed for any switching signal σ with ADT $\tau_a > \frac{\ln\mu}{\beta}$. The smooth switching LPV-PID controller can be constructed by (13)and (12).

Proof: According to (38) and (39), there is $X_j(\rho) + X_j^T(\rho) > 0$ guaranteed, which implies matrix $X_j(\rho)$ is non-singular. For subsets $\rho \in \Theta_i$, rewrite (38) in the form of (20) with

$$Z = \begin{bmatrix} \left\{ \begin{matrix} \mathrm{Her}\left(\bar{A}_i(\rho)Q_i(\rho)\right) \\ -\frac{\partial Q_i}{\partial \rho}\dot{\rho} + \beta Q_i(\rho) \end{matrix} \right\} & * & * & * \\ \bar{B}_{w,i}^T(\rho) & -\gamma I & * & * \\ \bar{C}_{z,i}(\rho)Q_i(\rho) & \bar{D}_{zw,i}(\rho) & -\gamma I & * \\ \bar{C}_{y,i}(\rho)Q_i(\rho) & \bar{D}_{y,i}(\rho) & 0 & 0 \end{bmatrix},$$

$$V = \begin{bmatrix} \bar{B}_{u,i}(\rho)M_i(\rho)X_i^{-1}(\rho) \\ 0 \\ \bar{D}_{zu,i}(\rho)M_i(\rho)X_i^{-1}(\rho) \\ -I \end{bmatrix}^T,$$

$$\Delta = \begin{bmatrix} X_i(\rho)\bar{C}_{y,i}(\rho) & 0 & 0 & \varepsilon X_i(\rho) \end{bmatrix}^T.$$

If N_V is chosen as

$$N_V = \begin{bmatrix} I & 0 & 0 & \bar{B}_{u,i}(\rho)M_i(\rho)X_i^{-1}(\rho) \\ 0 & I & 0 & 0 \\ 0 & 0 & I & \bar{D}_{zu,i}(\rho)M_i(\rho)X_i^{-1}(\rho) \end{bmatrix}^T, \tag{42}$$

according to Lemma 4, (38) is a sufficient condition for

$$\begin{bmatrix} \left\{ \begin{matrix} \mathrm{Her}(Q_i(\rho)A_{cl,i}(\rho)) \\ -\frac{\partial Q_i}{\partial \rho}\dot{\rho} + \beta Q_i(\rho) \end{matrix} \right\} & * & * \\ B_{cl,i}^T(\rho) & -\gamma I & * \\ C_{cl,i}(\rho)Q_i(\rho) & D_{cl,i}(\rho) & -\gamma I \end{bmatrix} < 0. \tag{43}$$

Then, multiply a diagonal matrix $diag[P_i(\rho), I, I]$ on both sides of (43), where $P_i(\rho) = Q_i^{-1}(\rho)$. By using Schur complement lemma, and substituting the controller expression in (13) and closed-loop system matrices in (18), (35) can be obtained, which is equivalent to (22) if a Lyapunov function is defined as

$$V_i(\rho, t) = \bar{x}^T P_i(\rho)\bar{x}.$$

Thus, from (38) we can obtain (22).

Similarly, if the Lyapunov function is defined as $V_{i,i+1}(\rho, t) = \bar{x}^T P_{i,i+1}(\rho)\bar{x}$ for $\rho \in \Theta_{i,i+1}$, from (39) we can obtain (23).

For the parameters on switching surfaces $\rho \in \Theta_i \cap \Theta_{i,i+1}$, the (40) implies that

$$\frac{1}{\mu}V_{i,i+1}(\rho, t) \le V_i(\rho, t) \le \mu V_{i,i+1}(\rho, t) \tag{44}$$

Therefore, all the criteria in Lemma 5 are satisfied.

Remark 8: Different from existing results [24], [25], [31], Theorem 7 only use the matrix variables $M_j(\rho)$ and $X_j(\rho)$ to construct the controller, and the Lyapunov matrices $Q_i(\rho)$ and $Q_{i,i+1}(\rho)$ are not involved. Thus, the Lyapunov functions for subsystems Θ_i and $\Theta_{i,i+1}$ can be designed independently.

Remark 9: Note that the matrix Δ in Lemma 4 has no constraints on its structure. While in Theorem 7, to obtain a convex synthesis condition, Δ is assumed as a block matrix only depending on the matrix variable $X_j(\rho)$. In other words, the convex synthesis condition in Theorem 7 is obtained by sacrificing part of the solution space. To make the solution space shrink less, a given parameter ε is included to scale $X_j(\rho)$ and explore more solution space. Consider a matrix N_Δ whose columns form the bases of the null space of Δ, where

$$N_\Delta = \begin{bmatrix} I & 0 & 0 & -\frac{1}{\varepsilon}\bar{C}_{y,i}^T(\rho) \\ 0 & I & 0 & 0 \\ 0 & 0 & I & 0 \end{bmatrix}.$$

pre- and post-multiply N_Δ and N_Δ^T on both sides of (38), and we get $N_\Delta Z N_\Delta^T < 0$ which implies

$$\begin{bmatrix} \Upsilon_1 & * & * \\ \bar{B}_{w,i}^T(\rho) & -\gamma I & * \\ \bar{C}_{z,i}(\rho)Q_i(\rho) & \bar{D}_{zw,i}(\rho) & -\gamma I \end{bmatrix} < 0, \tag{45}$$

where

$$\begin{aligned}
\Upsilon_1 = \mathrm{Her}\left(\bar{A}_i(\rho)Q_i(\rho)\right) - \frac{\partial Q_i}{\partial \rho}\dot{\rho} + \beta Q_i(\rho) \\
- \frac{1}{\varepsilon}Her\left[\bar{C}_{y,i}^T(\rho)\bar{C}_{y,i}(\rho)Q_i(\rho)\right]
\end{aligned}$$

Thus, the possibility of finding a feasible solution increases when the value of ε decreases.

Remark 10: In order to turn $\frac{\partial Q_i}{\partial \rho}\dot{\rho}$ to a practically valid constraint, the method in [4] is used. The differential term in (38) and (39) can be treated as $\sum_{i=1}^{s}\{\underline{\nu}_i, \overline{\nu}_i\}\frac{\partial Q_j(\rho)}{\partial \rho_i}$, where the notation $\sum_{i=1}^{s}\{\underline{\nu}_i, \overline{\nu}_i\}$ represents the combination of vertexes $\underline{\nu}_i$ and $\overline{\nu}_i$ for each parameter.

IV. APPLICATION TO FLIGHT CONTROL DESIGN

In this section, the longitudinal nonlinear model of F-16 aircraft is used in simulation to demonstrate the effectiveness of the proposed method. To achieve pitch-attitude hold and speed hold simultaneously, the control system is separated into two loops, one for attitude control and the other for speed control. The corresponding smooth switching LPV-PID controllers are designed for each loop.

A. LONGITUDINAL MODEL OF AIRCRAFT

The longitudinal motion of F-16 aircraft can be expressed as following nonlinear equations.

$$\begin{aligned}
\dot{V} &= \frac{T}{m_a}\cos\alpha - \frac{D}{m_a} - g\sin(\theta-\alpha),\\
\dot{\alpha} &= -\frac{T}{m_a V}\sin\alpha - \frac{L}{m_a V} + \frac{g}{V}\cos(\theta-\alpha) + q,\\
\dot{q} &= M/J_y,\\
\dot{\theta} &= q,\\
\dot{p}_a &= \frac{1}{\tau_{eng}}(p_c - p_a),
\end{aligned} \tag{46}$$

where m_a is the mass, g is the gravitational acceleration, V, α, q, θ, p_a are the airspeed, angle of attack, pitch rate, pitch angle, and engine power. p_c is the command of engine power which is a function of throttle setting δ_{th}. The dynamic model of the engine power is assumed as a first-order system, and τ_{eng} is the corresponding time constant which is a piecewise function depend on p_a and p_c. T is the thrust force which is a function of engine power p_a [32]. Drag D, lift L and pitch moment M can be expressed as

$$\begin{aligned}
D &= \bar{q}SC_D,\\
L &= \bar{q}SC_L,\\
M &= \bar{q}S\bar{c}C_m,
\end{aligned}$$

where

$$\begin{aligned}
C_D &= -C_{X_0}(\alpha,\delta_e)\cos\alpha - \left(\frac{q\bar{c}}{2V}\right)C_{X_q}(\alpha)\cos\alpha\\
&\quad - C_{Z_0}(\alpha)\sin\alpha + 0.19\left(\frac{\delta_e}{25}\right)\sin\alpha\\
&\quad - \left(\frac{q\bar{c}}{2V}\right)C_{Z_q}(\alpha)\sin\alpha,\\
C_L &= C_{X_0}(\alpha,\delta_e)\sin\alpha + \left(\frac{q\bar{c}}{2V}\right)C_{X_q}(\alpha)\sin\alpha\\
&\quad - C_{Z_0}(\alpha)\cos\alpha + 0.19\left(\frac{\delta_e}{25}\right)\cos\alpha\\
&\quad - \left(\frac{q\bar{c}}{2V}\right)C_{Z_q}(\alpha)\cos\alpha,\\
C_m &= C_{m_0}(\alpha,\delta_e) + \left(\frac{q\bar{c}}{2V}\right)C_{m_q}(\alpha)\\
&\quad + (x_{c.g.,ref} - x_{c.g.})C_Z.
\end{aligned} \tag{47}$$

$\bar{c}$ is the wing mean aerodynamic chord, $\bar{q}$ is the dynamic pressure, $x_{c.g.} = 0.3\bar{c}$ is the longitudinal centre of gravity, $x_{c.g.,ref} = 0.35\bar{c}$ is the reference longitudinal center of gravity, and S is the wing reference area. C_{X_0}, C_{Z_0}, C_{m_0}, C_{X_q}, C_{Z_q}, C_{m_q} are aerodynamic coefficients which can be obtained in the table of [33]. Table 1. lists the mass and geometry properties of F-16 aircraft.

TABLE 1. The mass and geometry properties of F-16 aircraft.

Parameter	m_a (lb)	J_y(slug $-$ ft^2)	$\bar{c}$ (ft)	S (ft^2)
Value	20500	55814	1.32	300

The above nonlinear aircraft model is difficult to be expressed as an explicit LPV model. To solve this issue, the gridding LPV modeling approach is used, which performs Jacobian linearization on the nonlinear model at each gridding point in the entire parameter space. If the gridding points are dense enough, the resulting LPV model can be considered as a good representation of the original nonlinear system, and the controller designed based on the LPV model can also guarantee the closed-loop system performance [34]. The scheduling parameter for the LPV model is selected as the airspeed because of its great influence on the system dynamics. The entire parameter space is set from 300 ft/s to 700 ft/s. It is partitioned into three subsets $\Theta_1 = \left\{\rho\in\Theta|\underline{\rho}_{1,1}\le\rho_1\le\bar{\rho}_{1,1}\right\}$, $\Theta_2 = \left\{\rho\in\Theta|\underline{\rho}_{2,1}\le\rho_1\le\bar{\rho}_{2,1}\right\}$, and $\Theta_{1,2} = \left\{\rho\in\Theta|\bar{\rho}_{1,1}\le\rho_1\le\underline{\rho}_{2,1}\right\}$ with $\underline{\rho}_{1,1} = 300$, $\bar{\rho}_{1,1} = 480$, $\underline{\rho}_{2,1} = 500$, $\bar{\rho}_{2,1} = 700$. The nonlinear model is linearized at every 30 ft/s in Θ_1 and Θ_2, and linearized at every 10 ft/s in $\Theta_{1,2}$. Thus, the LPV model of the aircraft can be expressed as

$$\begin{aligned}
\dot{x}_{air} &= A_{air,j}(\rho)x_{air} + B_{air,j}(\rho)u_{air},\\
y_{air} &= C_{air,j}x_{air},
\end{aligned} \tag{48}$$

This LPV model represents the perturbed dynamics of the aircraft about the gridding equilibrium points. The state x_{air}, control input u_{air} and output y_{air} are actually the small perturbations between the real and trimmed values. Without causing confusions, the notation of perturbation is omitted here for concise representation. In (48), the state $x_{air} = [\,V \quad \alpha \quad q \quad \theta \quad p_a\,]^T$, the input $u_{air} = \left[\,\delta_{th} \quad \delta_e\,\right]^T$, the output is $y_{air} = \left[\,p_a \quad V \quad \theta\,\right]^T$, and $y_{air} = \left[\,p_a \quad V \quad \theta\,\right]^T$.

The longitudinal model of rigid aircraft has a similar expression when the drag$D$, lift L, and pitch moment M are obtained. Thus, the LPV model in (48) can be used for other fixed-wing aircraft.

B. WEIGHTED SYSTEM INTERCONNECTION

The block diagram of the entire flight control system is shown in Fig.4, where the block "plant" is the longitudinal model of aircraft in (46). In this example, two autopilot systems are designed for pitch-attitude hold and speed hold. According

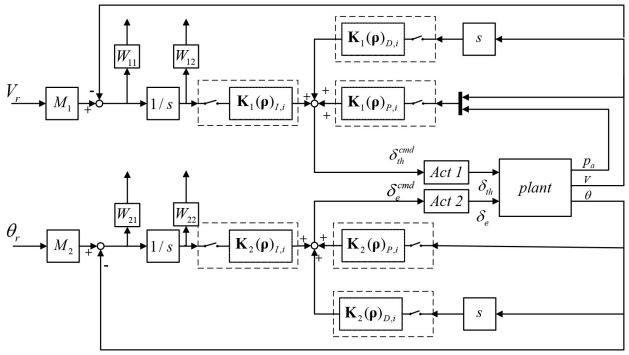

FIGURE 4. Flight control system interconnection.

to flight dynamics, the velocity is mainly controlled by the throttle, and the pitch attitude is controlled by the elevator.

To design these two autopilot systems, we rewrite the original linearized model given by (48) as two parts. One is the open-loop plant for velocity control, and the other is for attitude control. For the open-loop system for speed-hold, we select the throttle setting δ_{th} as the control input, and V and p_a as the states, because they are directly related to the velocity. The states α, q, θ are related to attitude, and they are together with the deflection of elevator δ_e considered as exogenous inputs. The LPV model of the velocity loop can be represented as

$$\begin{bmatrix} \dot{V} \\ \dot{p}_a \end{bmatrix} = A_{p1,j}(\rho) \begin{bmatrix} V \\ p_a \end{bmatrix} + B_{pw1,j}(\rho) \begin{bmatrix} \alpha \\ q \\ \theta \\ \delta_e \end{bmatrix} + B_{pu1,j}(\rho)\delta_{th},$$
$$\begin{bmatrix} V \\ p_a \end{bmatrix} = C_{p1,j} \begin{bmatrix} V \\ p_a \end{bmatrix}. \tag{49}$$

Similarly, for the open-loop system for pitch-attitude hold, we select the elevator angle δ_e as the control input, the angle of attack α, pitch rate q, and pitch angle θ as states. The airspeed V, engine power p_a and throttle setting δ_{th} are considered as exogenous inputs. The expression of this open-loop system is

$$\begin{bmatrix} \dot{\alpha} \\ \dot{q} \\ \dot{\theta} \end{bmatrix} = A_{p2,j}(\rho) \begin{bmatrix} \alpha \\ q \\ \theta \end{bmatrix} + B_{pw2,j}(\rho) \begin{bmatrix} V \\ p_a \\ \delta_{th} \end{bmatrix} + B_{pu2,j}(\rho)\delta_e,$$
$$\theta = C_{p2,i} \begin{bmatrix} \alpha \\ q \\ \theta \end{bmatrix}. \tag{50}$$

For the rest of this paper, the expressions of (49) and (50) are no longer given separately. We use the following general form to represent them:

$$\dot{x}_p = A_{p,j}(\rho)x_p + B_{pw,j}(\rho)w_p + B_{pu,j}(\rho)u_p,$$
$$y = C_{p,j}x_p. \tag{51}$$

The generalized open-loop system in (9) is obtained by connecting the aircraft model with the corresponding actuator, ideal model and weighting functions as shown in Fig.4. The control commands are directly sent to the actuators "Act 1" and "Act 2", which are considered as first-order systems with time constant $\tau = 0.2$ s for the throttle and 0.05 s for the elevator. The general state-space form for each actuator can be written as

$$\dot{x}_{act} = A_{act}x_{act} + B_{act}u,$$
$$u_p = C_{act}x_{act}, \tag{52}$$

where $A_{act} = -1/\tau$, $B_{act} = 1/\tau$, $C_{act} = 1$, u is the control command determined by the control algorithm, and u_p is the actual control input sent to the aircraft. As shown in Fig. 4, $u = \delta_e^{cmd}$ or δ_{th}^{cmd}, $u_p = \delta_e$ or δ_{th}.

Two ideal models, M_1 and M_2, are included to achieve the desired tracking performance for two autopilot systems. The optimization objective is to minimize the error between the ideal output and measurement output, which is similar as the model reference adaptive control. The general state-space form of each ideal model can be expressed as

$$\dot{x}_m = A_m x_m + B_m r,$$
$$y_m = C_m x_m + D_m r, \tag{53}$$

where r is the reference input, which is V_r or θ_r as shown in Fig. 4. Here, the ideal model is considered as a second-order system with the damping ratio $\zeta = 0.7$, the natural frequency $\omega_n = 1$ rad/s in attitude control system, and $\zeta = 1$, $\omega_n = 1$ rad/s in speed control system. The state-space matrices can be written as

$$A_m = \begin{bmatrix} 0 & 1 \\ -\omega_n^2 & -2\zeta\omega_n \end{bmatrix}, \quad B_m = \begin{bmatrix} 0 \\ \omega_n^2 \end{bmatrix},$$
$$C_m = \begin{bmatrix} 1 & 0 \end{bmatrix}, \quad D_m = 0.$$

In order to obtain a better performance, weighting functions are included for control synthesis. The weighting functions W_{11} and W_{21} are used to restrict the output performance. The general state-space form can be represented as

$$\dot{x}_{w1} = A_{w1}x_{w1} + B_{w1}(y_m - Gy)$$
$$e_1 = C_{w1}x_{w1} + D_{w1}(y_m - Gy), \tag{54}$$

where G is the selection matrix which is $G = \begin{bmatrix} 1 & 0 \end{bmatrix}$ in speed control system, and $G = 1$ in attitude control system. The system matrices are obtained from the transfer function $W_{11}(s) = \frac{100(0.2s+1)}{25s+1}$ for attitude control system, and $W_{21}(s) = \frac{10(0.2s+1)}{25s+1}$ for speed control system.

The weighting functions W_{12} and W_{22} are included to place a restriction on the integral of the tracking error, and thus limit the steady-state error. This weighting function is assumed as a constant, i.e.,

$$e_2 = D_{w2}x_I. \tag{55}$$

In our case, the dynamics of the integral term for PID controller is assumed as

$$\dot{x}_I = y_m - Gy. \tag{56}$$

TABLE 2. The constants for controller synthesis.

	μ	β	ε
Speed control loop	1.2	0.01	0.001
Attitude control loop	1.2	0.01	0.1

The generalized open-loop system is thus given as (57), shown at the bottom of the page, where $\bar{x} = \begin{bmatrix} x_p^T & x_{act}^T & x_m^T & x_{w1}^T & x_I^T \end{bmatrix}^T$, $w = \begin{bmatrix} w_p^T & r^T \end{bmatrix}^T$.

Because the above expressions are a general expression of velocity or attitude open-loop system, the smooth switching LPV-PID controllers can be constructed by using Theorem 1 for both systems. For the synthesis of the controller, the matrix variables are assumed parameter-dependent. Considering the computational complexity, first-order linear functions are used in our case. The matrices $M_{i,0}$, $M_{i,1}$, $X_{i,0}$, $X_{i,1}$, $Q_{i,0}$, $Q_{i,1}$, $Q_{i,i+1,0}$, $Q_{i,i+1,1}$, $i = 1, 2$ are the new variables to be solved. The first-order function is formulated as,

$$R_i(\rho) = R_{i,0} + \rho_1 R_{i,1}. \tag{58}$$

where $R_{i,0}$ and $R_{i,1}$ represent the above matrix variables. The control gains are calculated by (13) and (12).

C. NONLINEAR SIMULATIONS AND DISCUSSIONS

The proposed smooth switching LPV-PID control method is compared with the traditional ADT switching LPV-PID control method, for which the problem setup and synthesis conditions are given in Appendix. Here, these two methods are called "smooth switching" and "ADT switching" for short. For smooth switching, there are three adjacent subspaces $\Theta_1 = \{\rho \in \Theta | 300 \text{ ft/s} \leq \rho_s \leq 480 \text{ ft/s}\}$, $\Theta_2 = \{\rho \in \Theta | 500 \text{ ft/s} \leq \rho_s \leq 700 \text{ ft/s}\}$ and $\Theta_{1,2} = \{\rho \in \Theta | 480 \text{ ft/s} \leq \rho_1 \leq 500 \text{ ft/s}\}$, where the gains of controller switch smoothly in the transition subspace $\Theta_{1,2}$. For ADT switching, there are two adjacent subspaces $\Theta_1 = \{\rho \in \Theta | 300 \text{ ft/s} \leq \rho_1 \leq 490 \text{ ft/s}\}$, $\Theta_2 = \{\rho \in \Theta | 490 \text{ ft/s} \leq \rho_1 \leq 700 \text{ ft/s}\}$, and the switching happens on the surface $\rho = 490$ ft/s. The constants for controller synthesis are given in Table 2, and the optimized results of γ are shown in Table 3. It can be seen that these two methods achieve a similar performance level in terms of the value of γ.

Two nonlinear simulations with different reference signals are conducted to further test the performance. In case 1,

TABLE 3. The optimized parameter γ for control loops.

	Speed hold	Attitude hold
Smooth switching	198.675	115.984
ADT switching	169.773	115.984

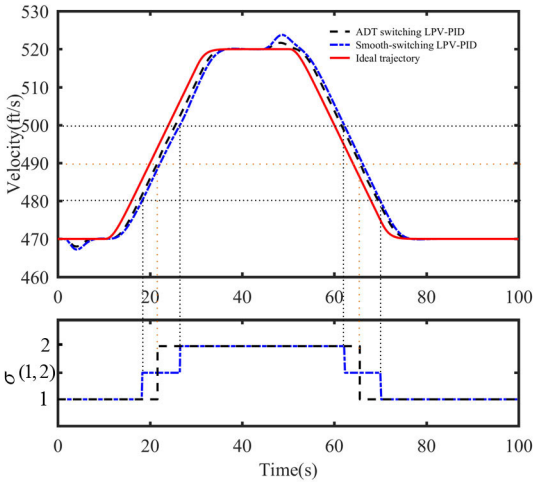

FIGURE 5. Actual and ideal trajectories of the airspeed for case 1.

the velocity command increases from 470 ft/s to 520 ft/s during the time period between 10 s and 30 s, and then decreases from 520 ft/s to 470 ft/s between 50 s and 70 s. The pitch angle command increases 10 degrees at 1 s, and decreases 10 degrees at 44 s. According to the ideal velocity trajectory shown in Fig. 5, switches occur at about 22 s and 67 s for the ADT switching method, and the transition processes for the proposed smooth switching method are roughly from 18 s to 25 s and from 63 s to 70 s. The overall speed tracking performance for both methods are acceptable as shown in Fig. 5.

In Fig. 6, the control input δ_{th} for ADT switching control has a big shaking at 22 s, which leads to the input saturation, and at 67s, small oscillations and saturation can also be observed. However, the control input δ_{th} for smooth switching control changes smoothly, and does not cause the actuator saturation. Note that the shaking of control inputs as shown in ADT switching is caused by the discontinuous control gains. To verify this, control gains are plotted as shown in Fig. 7 to visualize their variations with respect to time. The values of control gains for smooth switching vary continuously, while

$$\begin{aligned}
\dot{\bar{x}} &= \begin{bmatrix} A_{p,j}(\rho) & B_{pu,j}(\rho)C_{act} & 0 & 0 & 0 \\ 0 & A_{act} & 0 & 0 & 0 \\ 0 & 0 & A_m & 0 & 0 \\ -B_{w1}GC_{p,j} & 0 & B_{w1}C_m & A_{w1} & 0 \\ -GC_{p,j} & 0 & C_m & 0 & 0 \end{bmatrix} \bar{x} + \begin{bmatrix} B_{pw,j}(\rho) & 0 \\ 0 & 0 \\ 0 & B_m \\ 0 & B_{w1}D_m \\ 0 & D_m \end{bmatrix} w + \begin{bmatrix} 0 \\ B_{act} \\ 0 \\ 0 \\ 0 \end{bmatrix} u, \\
y &= \begin{bmatrix} -D_{w1}GC_{p,j} & 0 & D_{w1}C_m & C_{w1} & 0 \\ 0 & 0 & 0 & 0 & D_{w2} \end{bmatrix} \bar{x} + \begin{bmatrix} 0 & D_{w1}D_m \\ 0 & 0 \end{bmatrix} w,
\end{aligned} \tag{57}$$

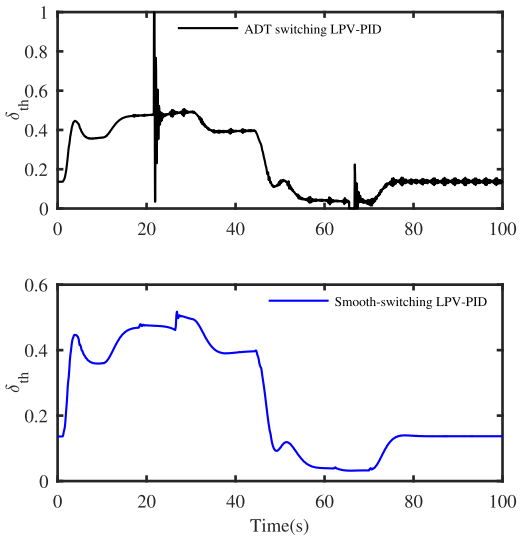

FIGURE 6. Throttle settings of the aircraft for case 1.

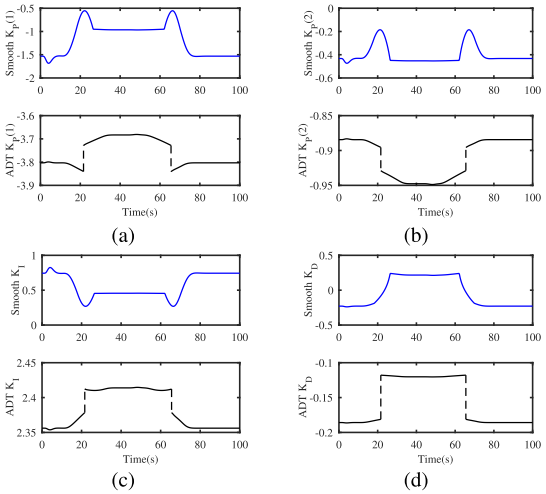

FIGURE 7. Variations of control gains for speed control loops in case 1.

those for ADT switching have discontinuous changes at 22 s and 67 s. Although all the control gains have small values, they can still lead to suddenly changed control commands when multiplying with large output feedbacks and integral of errors.

Fig. 8 gives a close look at the tracking errors. It shows that ADT switching control method generates a smaller tracking error. But when the speed command hits the switching surfaces, the big variation of the throttle will cause the actuator saturation, and the error will increase. To avoid this issue and simultaneously achieve an acceptable tracking performance, the smooth switching control might be a better choice. In addition, two overshoots in the velocity response around 5 s and 50 s are shown in Fig. 5 because the pitch angle changes at those instants, and the speed and pitch attitude autopilot systems are coupled.

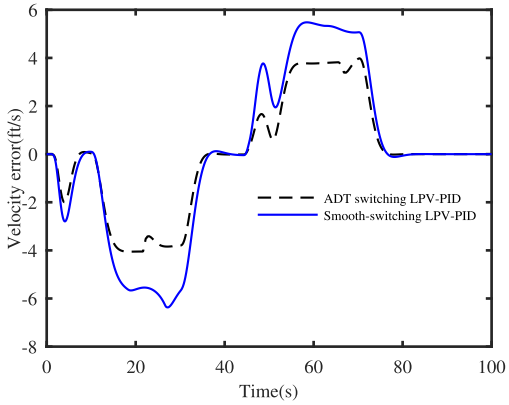

FIGURE 8. Tracking errors of the airspeed for case 1.

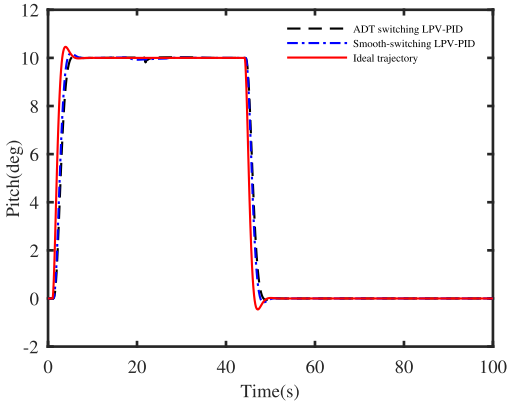

FIGURE 9. Actual and ideal trajectories of the pitch angle for case 1.

Fig. 9 shows the actual and ideal pitch angle trajectories. Because the controllers have the same switching strategy as the speed control loop, the switching also happens at 22 s and 67 s for ADT control. A small spike can be observed at 22 s for ADT switching, not for the smooth switching control. Correspondingly, the control input δ_e oscillates at 22 s for ADT switching, as shown in Fig. 10. But the smooth switching control method generates a much smoother control input with smaller oscillations. The control gains for the attitude control loop are also provided in Fig. 11, and the discontinuity of the ADT switching control gains can be observed. The tracking errors in Fig. 12 show that the ADT switching and smooth switching have similar tracking performances.

The second nonlinear simulation is performed to test the influence of the average dwell-time on the smooth switching performance. The reference signal of speed is designed switching fast at the beginning, and the dwell-times are shorter than the average dwell-time in this period. Then, slower switches are designed to compensate for the average dwell-time. As shown in Fig. 13, the switching times instants are 13 s, 18 s, 25 s, 28 s, 55 s, and 93 s. It can be seen that the switching system can maintain the stability as long as the overall average dwell time satisfies the requirement. The reference signal for the attitude control loop is 0 degree, and

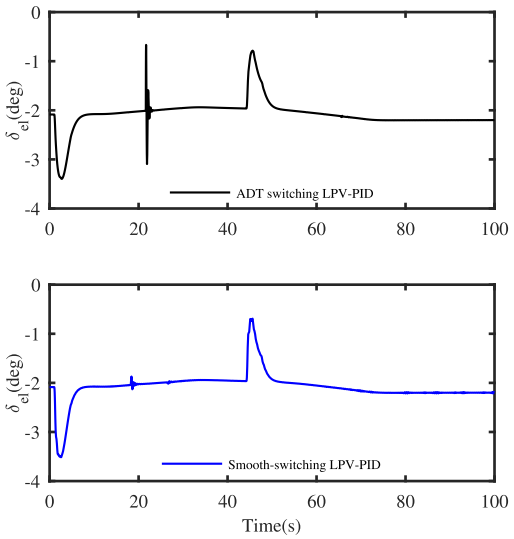

FIGURE 10. Elevator deflections of the aircraft for case 1.

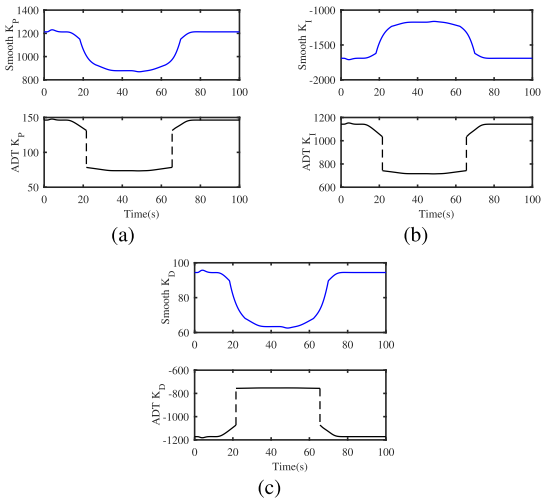

FIGURE 11. Variations of control gains for attitude control loops in case 1.

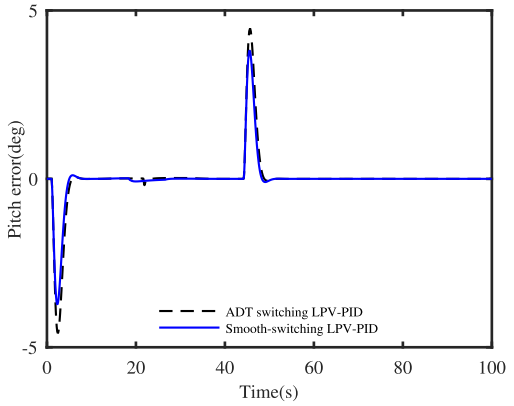

FIGURE 12. Tracking errors of the pitch angle for case 1.

the actual attitude trajectory is shown in Fig. 14. When the speed is changing, the attitude has some very small variations. It is because the influence of speed on the attitude control loop

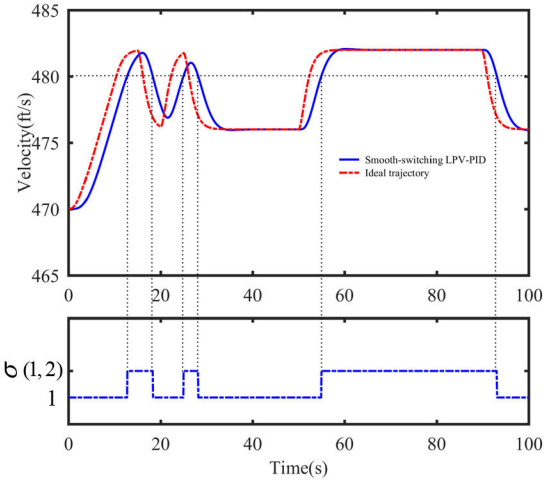

FIGURE 13. Actual and ideal trajectories of the airspeed for case 2.

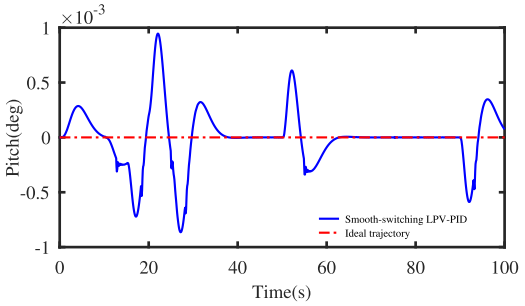

FIGURE 14. Actual and ideal trajectories of the pitch angle for case 2.

TABLE 4. The optimized parameter γ for the speed control loop with $\varepsilon = 0.001$.

μ	β	τ_a(s)	γ
1.2	0.005	36.46	195.82
1.2	0.01	18.23	198.67
1.2	0.05	3.65	256.57
1.05	0.01	4.87	200.13
1.3	0.01	26.24	198.17

TABLE 5. The optimized parameter γ for the attitude control loop with $\varepsilon = 0.1$.

μ	β	τ_a(s)	γ
1.2	0.005	36.46	108.17
1.2	0.01	18.23	115.98
1.2	0.05	3.65	infeasible
1.05	0.01	4.87	115.98
1.3	0.01	26.24	115.98

is considered as the disturbance when constructing the control system.

Finally, different values of μ and β are selected in controller synthesis to discuss their influences on the optimized parameter γ. Each control loop has five cases studied, and the value of ε is selected as 0.001 for the speed control and

0.1 for the attitude control. The results are listed in Table 4 and Table 5. Comparing with μ, β has a greater influence on the optimization result, and a large β value may cause the problem infeasible.

V. CONCLUSION

This paper presents a smooth switching gain scheduled PID control strategy for LPV systems. The controller is designed to have the smooth switching ability in the transition subspaces between neighboring LPV subsystems. The constraints for multiple parameter-dependent Lyapunov functions are derived for the closed-loop system with an ADT switching signal to guarantee stability and weighted L_2-gain performance. Based on these constraints and applying Finsler's lemma, the synthesis condition is formulated as an optimization problem subjected to LMI constraints. The proposed control strategy is applied to F-16 aircraft. Comparing with the traditional ADT switching, the proposed method can achieve smooth control commands and transition performance. In this way, the risk of saturation or mechanical wear of actuators can be reduced. Note that the system parameters are assumed to be accurate in this paper, and more complicated situations will be studied further in our future work, for example, control synthesis with external disturbances and parametric uncertainties, etc. In addition, the proposed method will be compared with other switching approaches, such as adaptive mixing control, and we will also explore the applicability of the proposed switching logic to adaptive control of switched systems.

APPENDIX

The ADT switching LPV-PID controller has the same expression as (5), but without smoothing part that is given by (16) and (17). The parameter space is divided into m parts as shown in Fig. 15. The switching occurs when the parameter trajectory hits a switching surface. The following is the synthesis condition for ADT switching LPV-PID control.

Theorem 11: Consider the open-loop system in (4), if there exist parameter dependent symmetric positive-definite matrices $Q_i(\rho) \in \mathbb{R}^{(n+ni)\times(n+ni)}$, full matrices $M_i(\rho) \in \mathbb{R}^{n_u\times n_{\bar{y}}}$ and $X_i(\rho) \in \mathbb{R}^{n_{\bar{y}}\times n_{\bar{y}}}$, scalars $\beta > 0$, $\mu > 1$, $\varepsilon > 0$ and $\gamma > 0$, such that the following optimization problem with LMI constraints

$$\min \gamma, \tag{59}$$

$$\Pi_i < 0, \rho \in \Theta_i, \tag{60}$$

$$\frac{1}{\mu}Q_{i,i+1}(\rho) \le Q_i(\rho) \le \mu Q_{i,i+1}(\rho), \ \rho \in \Theta_i \cap \Theta_{i+1}, \tag{61}$$

is solvable for any scheduling parameter ρ, where $i = \{1, 2, \ldots, m\}$is the index of subspaces. Then, the closed-loop system with the switching controller (5) is asymptotically stable for any switching signal σ with ADT $\tau_a > \frac{\ln\mu}{\beta}$ and the weighted L_2-gain performance $\gamma\mu^{N_0/2}$ guaranteed. The switching LPV-PID controller can be constructed by (13)and (12).

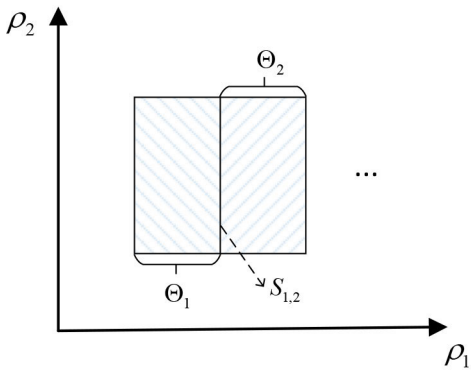

FIGURE 15. Partition of the traditional ADT switching parameter space along one axis.

ACKNOWLEDGMENT

The authors would like to thank anonymous referees and editors for their helpful comments and suggestions.

REFERENCES

[1] C. Hoffmann and H. Werner, "A survey of linear parameter-varying control applications validated by experiments or high-fidelity simulations," *IEEE Trans. Control Syst. Technol.*, vol. 23, no. 2, pp. 416–433, Mar. 2015.
[2] G. Becker and A. Packard, "Robust performance of linear parametrically varying systems using parametrically-dependent linear feedback," *Syst. Control Lett.*, vol. 23, no. 3, pp. 205–215, Sep. 1994.
[3] P. Gahinet and P. Apkarian, "A linear matrix inequality approach to H_∞ control," *Int. J. Robust Nonlinear Control*, vol. 4, no. 4, pp. 421–448, 1994.
[4] F. Wu, X. H. Yang, A. Packard, and G. Becker, "Induced L_2 norm control for LPV systems with bounded parameter variation rates," *Int. J. Robust Nonlinear Control*, vol. 6, nos. 9–10, pp. 983–998, 1996.
[5] B. Lu, F. Wu, and S. Kim, "Switching LPV control of an F-16 aircraft via controller state reset," *IEEE Trans. Control Syst. Technol.*, vol. 14, no. 2, pp. 267–277, Mar. 2006.
[6] L. Wu, X. Yang, and F. Li, "Nonfragile output tracking control of hypersonic air-breathing vehicles with an LPV model," *IEEE/ASME Trans. Mechatronics*, vol. 18, no. 4, pp. 1280–1288, Aug. 2013.
[7] T. He, G. G. Zhu, S. S.-M. Swei, and W. Su, "Smooth-switching LPV control for vibration suppression of a flexible airplane wing," *Aerosp. Sci. Technol.*, vol. 84, pp. 895–903, Jan. 2019.
[8] Y. Dai, L. Yu, J. Song, L. Abi, and S. Zheng, "Aircraft ground braking assistant control based on pilot control model," *IEEE Access*, vol. 8, pp. 88643–88650, 2020.
[9] V. F. Montagner, R. C. Oliveira, V. J. Leite, and P. L. Peres, "LMI approach for H_∞ linear parameter-varying state feedback control," *IEE Proc., Control Theory Appl.*, vol. 152, no. 2, pp. 195–201, 2005.
[10] P. Apkarian, P. Gahinet, and G. Becker, "Self-scheduled H_∞ control of linear parameter-varying systems: A design example," *Automatica*, vol. 31, no. 9, pp. 1251–1261, Sep. 1995.
[11] P. Apkarian and P. Gahinet, "A convex characterization of gain-scheduled H_∞ controllers," *IEEE Trans. Autom. Control*, vol. 40, no. 5, pp. 853–864, May 1995.
[12] F. Zheng, Q.-G. Wang, and T. H. Lee, "On the design of multivariable PID controllers via LMI approach," *Automatica*, vol. 38, no. 3, pp. 517–526, Mar. 2002.
[13] B. Carvalho and L. Rodrigues, "Multivariable PID synthesis via a static output feedback LMI," in *Proc. IEEE 58th Conf. Decis. Control (CDC)*, Dec. 2019, pp. 8398–8403.
[14] V. Veselý and A. Ilka, "Generalized robust gain-scheduled PID controller design for affine LPV systems with polytopic uncertainty," *Syst. Control Lett.*, vol. 105, pp. 6–13, Jul. 2017.
[15] M. S. Sadabadi and D. Peaucelle, "From static output feedback to structured robust static output feedback: A survey," *Annu. Rev. Control*, vol. 42, pp. 11–26, 2016.
[16] M. Mattei, "Robust multivariable PID control for linear parameter varying systems," *Automatica*, vol. 37, no. 12, pp. 1997–2003, Dec. 2001.

[17] A. Kwiatkowski, H. Werner, J. P. Blath, A. Ali, and M. Schultalbers, "Linear parameter varying PID controller design for charge control of a spark-ignited engine," *Control Eng. Pract.*, vol. 17, no. 11, pp. 1307–1317, Nov. 2009.
[18] A. Zandi Nia and R. Nagamune, "Switching gain-scheduled proportional–integral–derivative electronic throttle control for automotive engines," *J. Dyn. Syst., Meas., Control*, vol. 140, no. 7, Jul. 2018, Art. no. 071015.
[19] B. Lu and F. Wu, "Switching LPV control designs using multiple parameter-dependent Lyapunov functions," *Automatica*, vol. 40, no. 11, pp. 1973–1980, Nov. 2004.
[20] Y. Huang, C. Sun, C. Qian, and L. Wang, "Linear parameter varying switching attitude control for a near space hypersonic vehicle with parametric uncertainties," *Int. J. Syst. Sci.*, vol. 46, no. 16, pp. 3019–3031, Dec. 2015.
[21] D. Yang, G. Zong, and H. R. Karimi, "H_∞ refined antidisturbance control of switched LPV systems with application to aero-engine," *IEEE Trans. Ind. Electron.*, vol. 67, no. 4, pp. 3180–3190, Apr. 2020.
[22] P. Zhao and R. Nagamune, "Switching linear parameter-varying control with improved local performance and optimized switching surfaces," *Int. J. Robust Nonlinear Control*, vol. 28, no. 10, pp. 3403–3421, Jul. 2018.
[23] W. Wu, W. Xie, and L. Li, "Switching linear parameter-varying controller design with H_∞ performance based on youla parameterization," *IEEE Access*, vol. 8, pp. 184765–184773, 2020.
[24] P.-C. Chen, "The design of smooth switching control with application to V/STOL aircraft dynamics under input and output constraints," *Asian J. Control*, vol. 14, no. 2, pp. 439–453, Mar. 2012.
[25] W. Jiang, C. Dong, and Q. Wang, "Smooth switching linear parameter-varying control for hypersonic vehicles via a parameter set automatic partition method," *IET Control Theory Appl.*, vol. 9, no. 16, pp. 2377–2386, Oct. 2015.
[26] M. Hanifzadegan and R. Nagamune, "Smooth switching LPV controller design for LPV systems," *Automatica*, vol. 50, no. 5, pp. 1481–1488, May 2014.
[27] D. Yang, G. Zong, S. K. Nguang, and X. Zhao, "Bumpless transfer H_∞ anti-disturbance control of switching Markovian LPV systems under the hybrid switching," *IEEE Trans. Cybern.*, pp. 1–13, 2020, doi: 10.1109/TCYB.2020.3024988.
[28] G. Zhai, B. Hu, K. Yasuda, and A. N. Michel, "Disturbance attenuation properties of time-controlled switched systems," *J. Franklin Inst.*, vol. 338, no. 7, pp. 765–779, Nov. 2001.
[29] J. P. Hespanha and A. S. Morse, "Stability of switched systems with average dwell-time," in *Proc. 38th IEEE Conf. Decis. Control*, vol. 3, no. 12, 1999, pp. 2655–2660.
[30] M. C. de Oliveira and R. E. Skelton, "Stability tests for constrained linear systems," in *Perspectives in Robust Control*. Cham, Switzerland: Springer, 2001.
[31] L. Song and J. Yang, "Smooth switching output tracking control for LPV systems," *Asian J. Control*, vol. 14, no. 6, pp. 1710–1716, Nov. 2012.
[32] F. Garza and E. A. Morelli, "A collection of nonlinear aircraft simulations in MATLAB," *Tech. Memorandum*, vol. 212145, no. 1, pp. 1–92, 2003.
[33] L. T. Nguyen, *Simulator Study Stall/Post-Stall Characteristics a Fighter Airplane With Relaxed Longitudinal Static Stability*, Nat. Aeronaut. Space Admin., Washington, DC, USA, 1979, vol. 12854.
[34] A. K. Al-Jiboory, G. Zhu, S. S.-M. Swei, W. Su, and N. T. Nguyen, "LPV modeling of a flexible wing aircraft using modal alignment and adaptive gridding methods," *Aerosp. Sci. Technol.*, vol. 66, pp. 92–102, Jul. 2017.

BIXUAN HUANG received the B.S. degree from the School of Automation, Harbin Engineering University, China, in 2009, and the M.S. degree from the College of Information Science and Engineering, Northeastern University, China, in 2015. She is currently pursuing the Ph.D. degree with the School of Aeronautics and Astronautics, Shanghai Jiao Tong University (SJTU), China. Her research interests include reduced order control and linear parameter-varying control and application.

BEI LU received the B.S. and M.S. degrees in power and mechanical engineering from Shanghai Jiao Tong University (SJTU), China, in 1996 and 1999, respectively, and the Ph.D. degree in mechanical engineering from North Carolina State University, in 2004. From 2005 to 2017, she was a Professor with the Department of Mechanical and Aerospace Engineering, California State University Long Beach. She is currently a Professor with the School of Aeronautics and Astronautics, SJTU. Her main research interests include robust control, linear parameter-varying control, and application of advanced control and optimization techniques to aerospace, mechanical engineering problems.

QIFU LI received the B.S. and M.S. degrees in engineering mechanics from the Harbin Institute of Technology, in 1993 and 1999, respectively, and the Ph.D. degree in mechanical engineering from North Carolina State University, in 2006. Since 2007, he has been a Project Engineer led research teams in industry. Since 2010, he has been an Adjunct Professor with California State University Long Beach. He joined Shanghai Jiao Tong University (SJTU), in 2017. He is currently a Research Fellow with the School of Aeronautics and Astronautics, SJTU. His research interests include flight dynamics and control, and smart materials and structures.

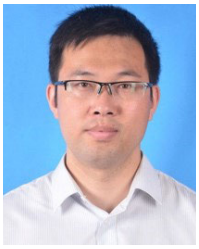

YANHUI TONG received the B.S. and M.S. degrees in automation and navigation, guidance and control from Northeastern University, Shenyang, China, in 2007 and 2009, respectively, and the Ph.D. degree in control science and engineering from the Space Control and Inertial Technology Center, Harbin Institute of Technology, China, in 2013. From November 2013 to September 2017, he worked as a Control System Engineer with the Shanghai Institute of Electro-Mechanical Engineering, Shanghai Academy of Spaceflight Technology, China. He is currently a Lecturer affiliated with the School of Electronic and Electrical Engineering, Shanghai University of Engineering Science, China. His research interests include switched system control, and model predictive control and their applications in flight control systems and industrial systems.